Chemisorption of C_2 Biradical and Acetylene on Reconstructed Diamond(111)-(2 × 1)

Shuo Wang Yang,[†,‡] Xianning Xie,[†] Ping Wu,[‡] and Kian Ping Loh*[,†]

Department of Chemistry, National University of Singapore, 3 Science Drive 3, Singapore, and Institute of High Performance Computing, Singapore

Received: June 5, 2002; In Final Form: November 6, 2002

We present converged first-principles calculations for the atomic and electronic structure of the diamond-(111)-(2 × 1) face adsorbed with C_2 or C_2H_2 based on the periodic density functional theory (DFT) in the general gradient approximation. The unique geometry of the C(111)-(2 × 1) Pandey chain provides the ideal molecular template for the self-assembly of C_2. Depending on the initial bonding configuration of the C_2 biradical on the Pandey chain, self-assembly via mutual interactions can result in different superstructures. The most stable C_2 binding site on the C(111)-(2 × 1) surface is the straddled bridging site between adjacent Pandey chains. Van der Waals Epitaxy of graphite can proceed on the C(111)-(2 × 1) template following the self-assembly of C_2 biradical, with consequent gain in surface energy. The self-assembly of C_2H_2 on top of the Pandey chain results in the formation of polyethylene that follows the zigzag course of the chain. The adsorption of C_2H_2 can passivate the surface states on C(111)-(2 × 1) and result in an opening of the surface band gap.

Introduction

Atomistic surface processes such as reconstructions and epitaxial growth can result in new material system in nanometer scale with unpredecented structural and electronic properties. Among such structures, the one-dimensional atomic chains, or surface quantum wires (SQW) formed by self organization during various adsorption and growth have received particular interest.[1] The one-dimensional (1-D) solids feature exotic phenomena such as Peierls instability, anomalous phonon dispersions, spin and charge density waves, and unconventional superconductivity. In recent years, many atomic-scale 1-D structures have been observed on metals, e.g., 1-D polymer-like reaction products with O_2/H_2 on Cu(110), Ag(110), and Ni(110).[2,3] In the case of semiconductors, another variety of 1-D chains include the missing dimer chains on the Ge/Si(001),[4] Bi wires on Si(001),[5] Si chains on SiC(001),[6,7] and C_2H_4 molecular chains on Si(001).[8]

The reconstructed diamond(111)-(2 × 1) face is an interesting candidate to find brand new 1-D materials due to the inherent low dimensionality as well as the weak interaction between the π reconstructed face and the adsorbate. We consider in this study adsorbate systems such as the C_2 biradical as well as C_2H_2 molecules. Both of these are gas-phase precursors which could contribute to diamond growth, and have been detected by various in-situ diagnostic means in previous studies.[9−14] Recently there has been intense interest in the preparation of ordered organic monolayes on Si(001) where the orientation of the individual organic molecule is influenced by the orientation of the underlying Si═Si dimer.[8,15,16] Alkenes for example can bond to the Si(001) surface by breaking the π bond of the alkene and the silicon (001) dimers, forming two sigma bonds. This process does not involve fragmentation and provides better control of atomic structure and assembly. Similar adsorption problems on diamond have not been studied.

The presence of C_2 has been detected in the CH_4/H_2 or C_{60} mixture used for diamond deposition as green Swan bands by optical emission spectroscopy, and has been correlated to diamond-like or nanocrystalline diamond deposition.[9−14,17−19] In terms of fundamental chemistry, the detection of C_2 radicals has led to the proposal of a new diamond growth process based on the insertion of C_2 on the dimer bridge site on the C(100) or C(110) surfaces.[20−22] It has been demonstrated that nanocrystalline diamond can be deposited in a hydrogen-poor environment (e.g., C_{60}/Ar) where C_2 is the main precursor.[9−14] The mechanism for the growth of nanocrystalline diamond films from C_2 radicals have been proposed for the C(100) and C(110) surfaces due to the availability of ready adsorption site on these surfaces for direct C_2 insertion.[20−22] Earlier density functional theory (DFT) calculations for C_2 insertion on the C(110) surface for example showed that the individual steps in this growth mechanism are energetically very favorable and have small activation barriers.[22]

To the best of our knowledge, no proposal for the propagation of the C(111) face based on direct C_2 addition has been proposed, despite the fact that the slow-growing (111) face has been observed to manifest as the dominant crystal habit during a large part of the diamond growth window prior to the degradation of the crystal habits into nanograins under a hydrogen-poor, C_2-rich growth conditions.

The reconstructed C(111)-(2 × 1) can be generated in a vacuum following the desorption of hydrogen from the surface at 900 °C. The Pandey π bonded chain is clearly favored on the surface although the precise positions of the atoms in the unit cell are still under debate.[23−25] The Pandey chain can be considered as a weakly bound quasi one-dimensional chain on the C(111)-(2 × 1) surface. The frontier orbitals of the carbon chain atoms consist of π bonding and π^* antibonding orbitals analogous to the structure of alkenes. It is possible that one-dimensional conductors of the "conjugated polymer" type can

* Corresponding author. E-mail: chmlohkp@nus.edu.sg. FAX: (65) 67791691.
† Department of Chemistry.
‡ Institute of High Performance Computing.

10.1021/jp021347m CCC: $25.00
Published on Web 01/07/2003

arise from the self-assembly of C_2 or C_2H_2 precursors *on* the Pandey chains, or *between* the chains where head-on interaction between the p orbitals of the adsorbate and the substrate allows σ bonding. Intramolecular π bonds can be formed in these polymer chains via delocalization of electrons in the p_z orbitals along the chain, but it remains to be investigated whether intrabonding within the chain is stronger than interbonding with the substrate. A quantum chain system can be formed if there is very weak substrate−chain interaction achieved via secondary p_z orbital interaction. In view of this, we need to address the possible bonding geometry of C_2 and C_2H_2 on the reconstructed C(111) face. The purpose of our investigation is to identify possible bonding geometries and pathways for the self-assembly of these species on the C(111) surface to see if thin superstructures that observe special epitaxial relationship to the substrate can be developed.

Experimental Procedures

Periodic DFT Calculations of Diamond Face. The total-energy calculations and optimizations were performed for all the clean C(111)-(1 × 1), C(111)-(2 × 1), and the chemisorbed C_2 and C_2H_2 systems using the plane-wave pseudopotential method (CASTEP) based on density-functional theory in the general gradient approach for exchange and correlation.[26,27] The Vanderbilt ultrasoft pseudopotentials were used.[28] The wave functions were expanded into plane waves up to an energy cutoff of 500 eV. Special k points generated according to Monkhorst−Pack scheme[29] were used for integration over the irreducible wedge of the Brillouin zone for the various surface structures, with k spacing of 0.05 $Å^{-1}$ for diamond(111)-(2 × 1) surface slab. The geometry optimizations were performed by the Broyden−Fletcher−Goldfarb−Shanno (BFGS) routine.[30] The exchange and correlation energies were calculated with the Perdew−Wang form of the generalized-gradient approximation (GGA-PW91).[31] The equilibrium lattice constant of 3.553 Å is obtained by optimizing the unit cell of bulk diamond. This value represents the experimental data of 3.567 Å with error of less than 0.4%. We used this lattice constant for all further surface computations.

The supercell method is used to calculate the diamond surface systems and molecular systems, where the crystal surface is represented by a thick slab (12 carbon layers) with a vacuum region (10 Å) and a molecule (such as C_2 or C_2H_2) is put in a large cubic box with a cell parameter of 10 Å. The bottom of the slab is saturated by H termination. The thickness of slabs and vacuum region has been tested to be large enough to avoid the interaction between the replicas.

The chemisorption energy ΔE_{ad} is calculated as

$$\Delta E_{ad} = E_{system} - E_{cleansurface} - E_{adsorbate}$$

where E_{system} refers to the total energy of the chemisorbed system, $E_{cleansurface}$ is the total energy of the clean C(111)-(2 × 1) surface, and $E_{adsorbate}$ is the total energy of the adsorbate.

Results

(i) C_2 and C_2H_2 Chemisorption Sites on Diamond(111). The optimization of the reconstructed C(111)-(2 × 1) was started from the ideal geometry proposed by Pandey.[23] This is a π bonded chain structure where atoms in the top two layers form chains with a bond length =1.425 Å, similar to the graphitic layer. Figure 1a,b shows the side view and top view of the zigzag Pandey chain running in the [$\bar{1}$10] direction. The electronic band structure of the relaxed C(111)-(2 × 1) Pandey

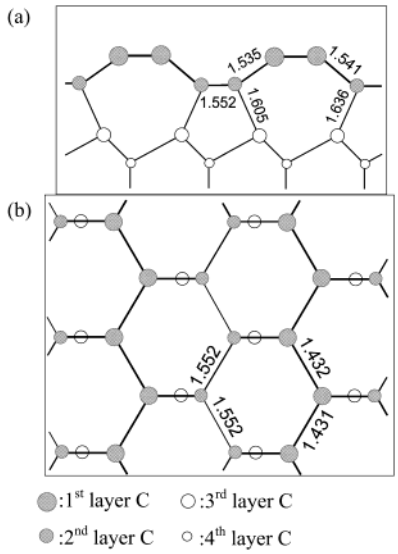

Figure 1. Reconstructed C(111)-(2 × 1) Pandey chain structure where atoms in the top two layers form chains with a bond length = 1.425 Å, similar to the graphitic layer. (a) and (b) shows the side view and top view of the zigzag Pandey chain.

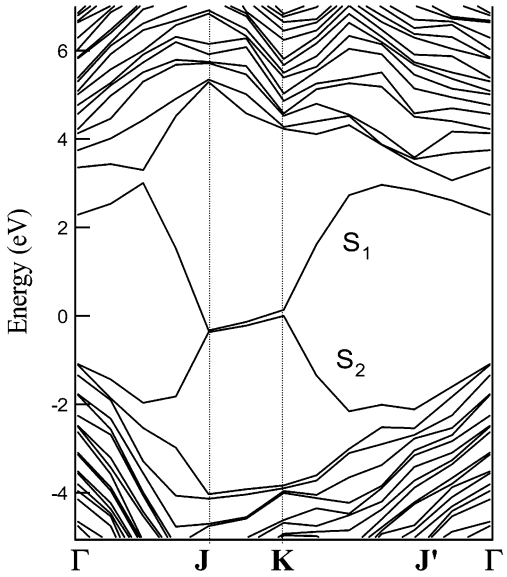

Figure 2. Band structure of the C(111)-(2 × 1) surface for Pandey π bonded chain geometry.

chain in Figure 2 shows mainly the occupied (S_2) and unoccupied surface bands (S_1) deriving from the π bonding and π^* antibonding combinations of the p orbitals along the chain and perpendicular to the surface. The nearly flat and degenerate bands along the $\overline{JK}$ indicates the one-dimensional nature of the chain. The very small upward dispersion of the chain suggests chain−substrate interactions. The closing of the surface band gap at the Fermi level makes the surface semimetallic and originates from the chemically equivalent atoms along the chain.

We consider a few possible chemisorption sites on the C(111)-(2 × 1) surface for the insertion of C_2 and C_2H_2, with a view in considering whether the chemisorbed species can become a surface site for the adsorption of a second layer to propagate a well-defined diamond face in a layer-by-layer mode, in such a case the process is classified as growth. The C_2 radical is a potential building block because it can generate the {110} and {111} diamond face by direct insertion into the growing sites to propagate diamond growth. For C_2H_2, further abstraction of the hydrogen by atomic hydrogen is necessary before the

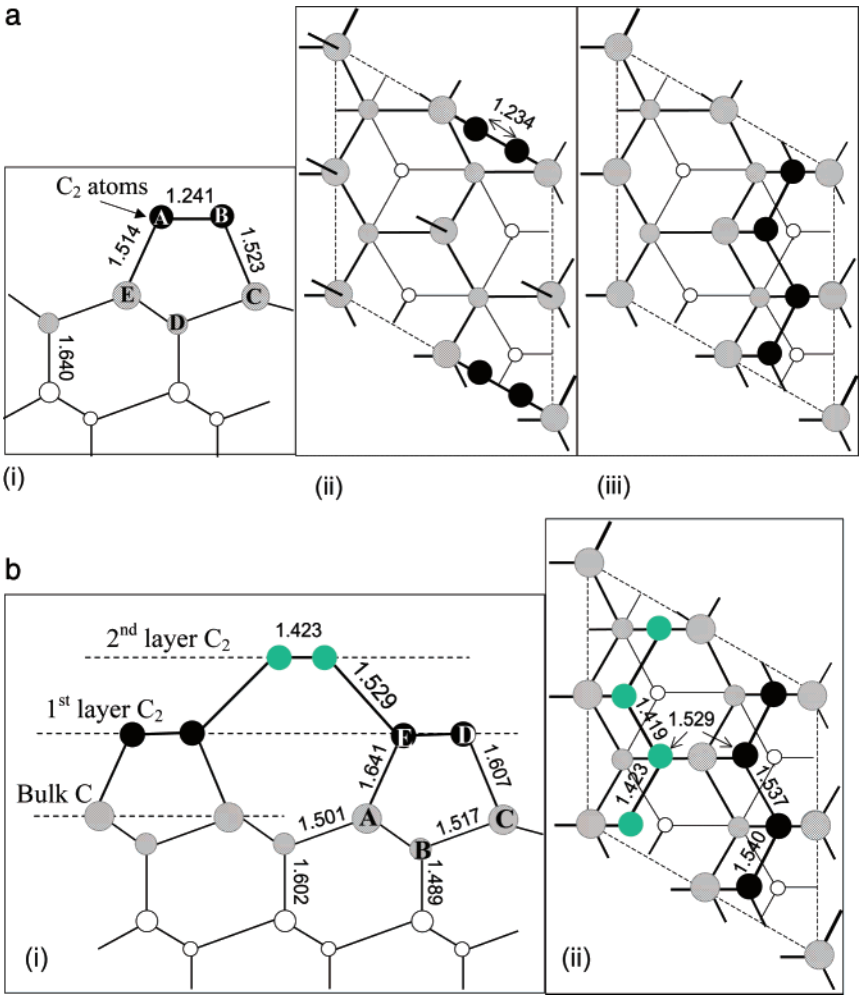

Figure 3. (a) Adsorption of C_2 biradical on the C(111)-(1 × 1) surface in a (2 × 2) unit cell, the C_2 is intentionally spaced apart in (i) and (ii), showing side view and top view respectively; (iii) the addition of another C_2 results in a zigzag chain upon optimization. (b) Addition of a second layer of C_2 on-top of the preadsorbed first layer on the C(111)-(1 × 1) surface gives rise to the C(111)-(2 × 1) surface.

carbon can be fully incorporated into the lattice. If the propagation of a well-defined face is not possible, then the chemisorbed species may constitute a new nucleation center and the process is classified as nucleation. The optimized bond length in C_2 and C_2H_2 was calculated to be 1.267 and 1.196 Å, respectively.

(ii) C_2 Chemisorption on C(111)-(1 × 1). For a single-bond cleavage (111)-(1 × 1) surface, the adsorption of C_2 on the dangling bonds of two surface carbon in the 1 × 1 unit cell yields a chemisorption energy of −3.91 eV per C_2. In this case, a (2 × 2) unit cell was considered intentionally to keep the position of the next-nearest neighbor vacant, as shown in Figure 3a.i,ii. The optimized structure at first consists of the C_2 aligned with the edge of the (1 × 1) unit cell. The adsorption of a second C_2 on the nearest-neighbor site is exothermic by 9.2 eV/mol, enhanced by lateral interaction among the neighboring C_2 such that the equilibrium structure produces a zigzag chain running in the [$\bar{1}$10] direction, as shown in Figure 3a.iii. The side view of a five-member ring structure (ABCDE) as shown in Figure 3a.i reveals that the zigzag chain structure is similar to the second carbon layer of the reconstructed C(111)-(2 × 1) surface. The first layer of the C(111)-(2 × 1) can be generated by the addition of a second layer of C_2 on-top of the preadsorbed ones, as shown in Figure 3b.i, such that 5-fold and 7-fold rings are obtained underneath the surface by self-assembly. In other words, the adsorption of two layers of C_2 on the C(111)-(1 × 1) surface results in an equilibrium structure of a C(111)-(2 × 1) surface. The $C_{firstlayer}-C_{secondlayer}$ bond distance of 1.53 Å and $C_{secondlayer}-C_{thirdlayer}$ bond distance of 1.64 Å is similar to that of the optimized C(111)-(2 × 1) clean surface. Such layer-by-layer total energy calculations reveal that C_2 will self-assemble on the bulk-terminated face to result in the π bonded chain reconstruction.

(iii) C_2 Chemisorption on C(111)-(2 × 1). Next we consider the possible chemisorption sites on the C(111)-(2 × 1) for C_2. One possible chemisorption site is direct "on-top" insertion into the two carbon atoms within the Pandey chain. The intrachain insertion of C_2 could lead to carbene-type cyclopropylidene or cyclobutyne-like structure. If the C_2 was allowed to approach with its bond axis perpendicular to the surface, an erect cyclopropylidene structure is formed with a chemisorption energy of −3.58 eV per C_2 molecule per (2 × 1) unit cell, as shown in Figure 4. The C−C bond distances between the surface carbon and the nearest attached C_2 carbon is 1.47 Å and the C−C bond length between the carbon in the Pandey chain is 1.48 Å, such that the structure resembles a cyclopropylidene. The C−C bond length for the immediate sites not attached to the adsorbed C_2 has relaxed to 1.526 Å, which is close to the bulk values of 1.542 Å. No tilting of the C_1-C_2 bond axis with respect to the surface to facilitate lateral bonding between neighboring chemisorbed C_2 was found. This is judged to be a consequence of the very stable three-member triangular structure formed in the cyclopropylidene structure with bond angles close to that of an equilateral triangle (60°).

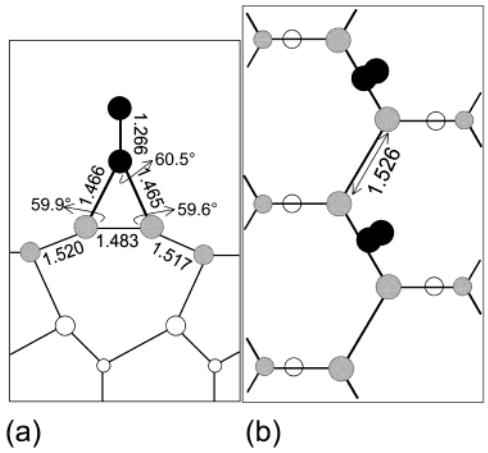

Figure 4. Optimized structure of C_2 chemisorption with its bond axis perpendicular to the C(111)-(2 × 1) surface, forming a cyclopropylidene: (a) side view and (b) top view. Chemisorption energy = −3.58 eV per C_2 per (2 × 1) unit cell.

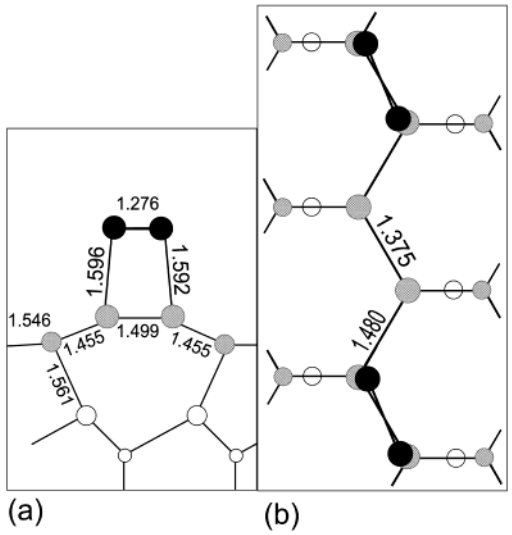

Figure 5. Optimized structure of cyclobutyne formed by the chemisorption of C_2 with its bond axis parallel to the Pandey chain, 50% surface coverage, (a) side view and (b) top view. Chemisorption energy = −2.26 eV per C_2 per (2 × 1) unit cell.

To see if a cyclobutyne-type structure can be formed, the C_2 radical was allowed to approach the surface with its bond axis parallel to the sample face. The situation of 50% coverage where the adsorbed C_2 was spaced out to prevent lateral interaction is shown in Figure 5. The C−C distance in the adsorbed C_2 is 1.276 Å, whereas the substrate C−C distance is 1.499 Å. The chemisorption energy of −2.26 eV per C_2 per (2 × 1) unit cell suggests that this is a less preferred bonding structure compared to the former case. The substrate−adsorbate distance was 1.596 and 1.592 Å, respectively. The strong substrate−adsorbate interaction can be judged from the lifting of the chemical equivalence of the Pandey Chain. The C−C distance of the unoccupied substrate site between the two adsorbed C_2 was shortened to 1.375 Å, indicating a greater degree of π bonding between substrate carbon that has not directly interacted with C_2. The C−C distance in the Pandey Chain alternates between 1.499 Å for the occupied and 1.480 and 1.375 Å for the unoccupied sites.

If the surface coverage of C_2 was increased to 100% in an attempt to form a conjugated, zigzag chain, an interesting situation results. It is found that no stable chemisorption between the C_2 chain and the substrate can occur because of the strong

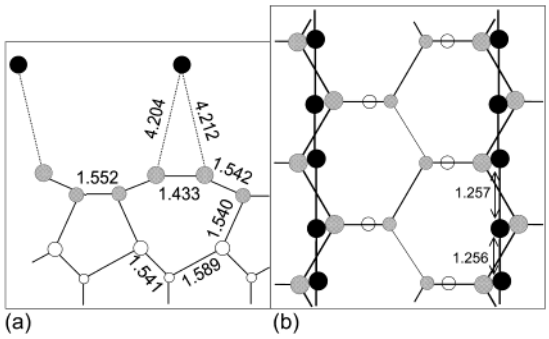

Figure 6. Formation of a quantum chain following the optimization of the surface structure consisting of a full coverage of C_2 in an "on-top" fashion on the Pandey chain, (a) side view and (b) top view.

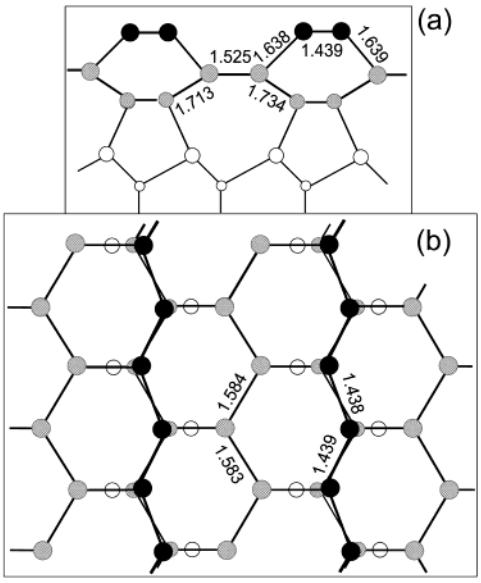

Figure 7. (a) Chemisorption of C_2 in a straddled fashion between the Pandey chain, showing the (a) top view (b) side view of the chemisorbed C_2. Note the formation of a six membered ring and the similarity of this surface to the C(110) surface. Chemisorption energy = −6.38 eV.

lateral interaction between the C_2 once the C_2 gets within lateral bonding distance. The optimized structure is a linear quantum chain that runs parallel to the direction of the Pandey chain with an isoequivalent bond distance of 1.256 Å, as shown in Figure 6. The equivalent intrachain distances suggest the delocalization of the p_z electrons along the chain. The substrate−chain distance is 4.204 Å (larger than van der Waals distance in graphite), so effectively this is out of the covalent or weak van der Waals bonding range between the chain and the substrate.

The third chemisorption site considered involved the bridging of the C_2 between the carbon of two neighboring Pandey chains running in the $[\bar{1}10]$ direction. The most stable configuration, as shown in Figure 7, adopts a straddled geometry between the two parallel Pandey chains, with the atomic positions of the two carbon atoms of the C_2 directly overlapping with the two carbons of the third layer. The bond axis of the C_2 in this case is aligned alternatively with the $[\bar{1}2\bar{1}]$ and $[2\bar{1}\bar{1}]$ directions. The chemisorption energy of −6.38 eV per C_2 indicates that this is the most stable configuration among all the C_2 sites considered. Lateral chemical interaction among the neighboring chemisorbed C_2 allows the propagation of a zigzag chain running in similar direction to the underlayer chain such that the (2 × 1) reconstruction of the underlayer is replicated by the overlayer formed by the C_2, as shown in Figure 7. The bridging bond

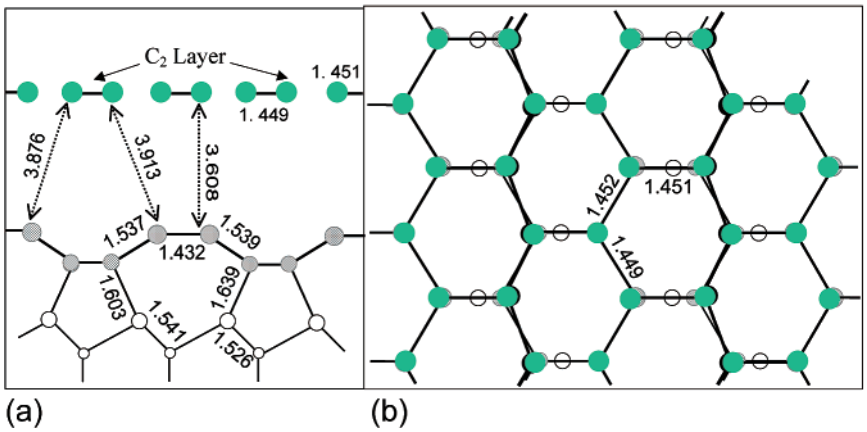

Figure 8. (a) Side and (b) top views of the epitaxial graphite formed by the chemisorption of a second layer of C_2 layer on top of the first layer C_2 shown in Figure 7. Chemisorption energy = −12 eV.

distances to the first layer substrate carbon are 1.63 Å. The C−C bonds in the substrate Pandey chain have relaxed from 1.421 to 1.525 Å. Interlayer bond distances have also expanded with the chemisorption of C_2, and a slight buckling is present with the bond distances between the second and third layer carbon increasing to 1.734 and 1.713 Å respectively. The side view of the structure as shown in Figure 7b shows that the subsurface ring which the overlayer C_2 belongs is a six-member ring (indicated as ABCDEF in Figure 7a), similar to the structure of the (110) face. In other words, the chemisorption of C_2 in a bridging fashion between two Pandey chain generates a "(110)-type" surface on-top of the C(111)-(2 × 1). It is interesting to consider whether the (110) face can propagate simply by the addition of C_2 in a similar "bridging-fashion" between the zigzag chain, allowing the "(110)-type" surface to grow from the C(111)-(2 × 1) template.

To investigate whether a second layer of C_2 can be added in a straddled geometry between the zigzag chain of the first layer of adsorbed C_2, we add another layer of C_2 between the chemisorbed C_2 chains. Following optimization, it was found that self-assembly of the C_2 structure due to strong lateral chemical interactions results in the formation of a graphite honeycomb structure with $C-C_{ring}$ = 1.45 Å. This graphite layer is epitaxially grown on top of the C(111)-(2 × 1) face because almost complete registry of it with the C(111)-(2 × 1) face is obtained, as viewed from the top in Figure 8. This is equivalent to the process of van der Waals Epitaxy, where the formation of sharp and defect-free interfaces between the 2D graphite and the 3D substrate occurred.[32,33] The distances between the graphite epilayer and the C(111)-(2 × 1) substrate of 3.61 Å is within the van der Waals bonding range. The heat of reaction generated from the addition of a second layer C_2 on the first layer to give the graphite epilayer is calculated to be −12 eV per C_2 per (2 × 1) unit cell. The exothermic heat or reaction suggests that diamond propagation on the C(111) face is inhibited by C_2 adsorption due to the tendency to self-assemble to form graphite. The increased corrugation of the C(111)-(2 × 1) surface provides a better matching to the flat graphite layer compared to the C(111)-(1 × 1) face. Therefore our results predict that growth conditions utilizing hydrogen-poor, C_2-rich gas feed easily result in the graphitization of the C(111) face following the self-assembly of C_2 in a layered fashion on the surface.

(iv) C_2H_2 Chemisortion site on C(111). In the case of C_2H_2 adsorption on (111)-(2 × 1), we consider first the direct addition on the zigzag chain. Initially the C_2H_2 was intentionally spaced out to prevent lateral interactions. If only isolated C_2H_2 adsorbs

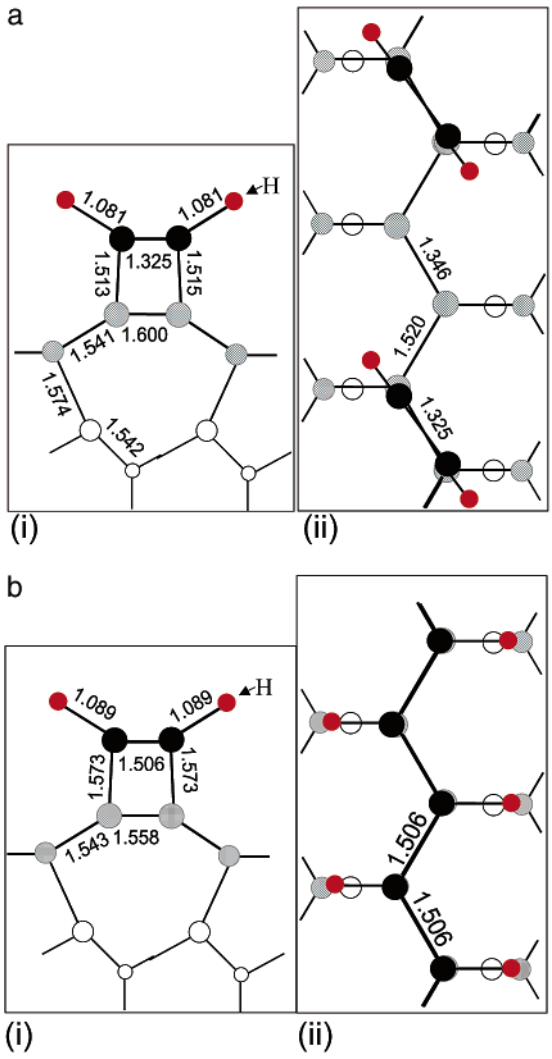

Figure 9. (a) (i) Side and (ii) top views of the cyclobutene structure formed by the chemisorption of C_2H_2 directly on top of the Pandey Chain at 50% coverage, chemisorption energy = −1.42 eV. (b) Chemisorption of C_2H_2 directly on top of the Pandey Chain at 100% coverage. Chemisorption energy = −2.26 eV, (i) side view and (ii) top-view.

on the chain to attain 50% coverage, a cyclobutyne-like structure is formed between the C_2H_2 and the substrate, as shown in Figure 9a. In this case the substrate C−C carbon that bonds directly with the acetylene is relaxed to 1.6 Å (from original 1.42 Å) and the neighboring C−C distances are changed to 1.52

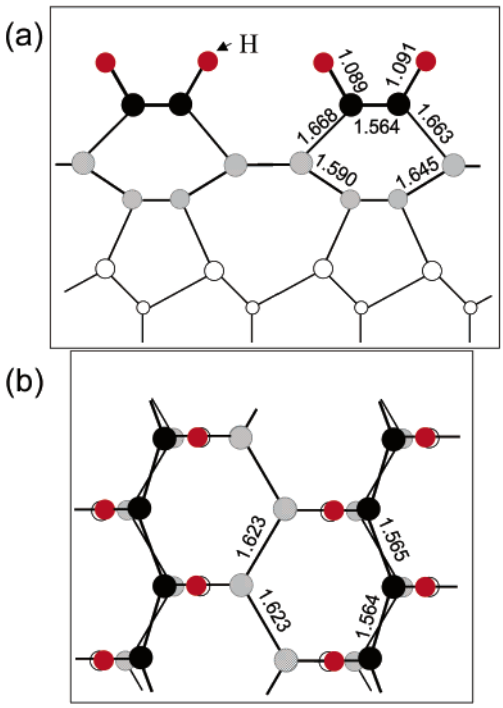

Figure 10. (a) Side and (b) top views of the cyclobutene structure formed by the chemisorption of C_2H_2 in a straddled configuration between two Pandey Chains. Chemisorption energy $=-1.76$ eV.

and 1.34 Å. The relaxation of one site causes the C−C bond distance in the next-nearest site to be constricted. The chemisorption energy is −1.42 eV.

If the coverage of C_2H_2 is increased to 100%, the geometry of the zigzag adsorption site favors the side-on overlap of the p orbital between adjacent C_2H_2. The side-on overlap allows the sp^3 rehybridization of the isolated cyclobutyne into polyethlyene, as shown in Figure 9b and relaxes the C−C bond. The plan view in Figure 9b.ii shows that the lateral interaction gives rise to a polyethylene chain that runs parallel to the Pandey chain. The breakages of two π bonds and formation of four sigma bonds are energetically favorable ($145 \times 2 - 4 \times 80$ kcal/mol). Consequently, the addition of C_2H_2 on the Pandey chain carbon gives rise to a self-assembled polyethylene structure with a substrate−adsorbate distance of 1.573 Å and an equivalent C−C bond distance of 1.506 Å (from 1.325 Å at 50% coverage case), and with a chemisorption energy of −2.26 eV per C_2H_2.

Another possible site is the binding of the C_2H_2 in a bridging fashion between two rows of Pandey chain. Self-assembly via lateral bonding can generate a polyethylene structure, as shown in Figure 10. In this case, the C−C bond distance has expanded to 1.564 Å. The chemisorption energy of −1.76 eV per C_2 per (2×1) unit cell suggests that the bridging structure is a less favorable option compared to the on-top structure. It is noteworthy that the reverse is true in the case of C_2 adsorption. No further assembly of another C_2H_2 adlayer on the preadsorbed layer is possible because the surface is effectively passivated following the rehybridization into sp^3 bonding.

(v) Density of States and Band Structure Calculation. One interesting result from the DFT study is the suggestion of the possibility of preparing a diamond/graphite, diamond/quantum chain, diamond/C_2H_2 superstructure by the assembly of C_2 and C_2H_2 on the C(111)-(2×1) surface. Charge transfer between the adlayer and the substrate can be judged from the changes in the surface DOS of the substrate before and after the chemisorption. The layered-resolved DOS of clean diamond (2×1) surface shows that the DOS of the surface-states in the bulk-gap is mainly concentrated on the topmost layer, as shown in Figure 11. The DOS of the surface-states in the bulk gap extends over the entire region from 0 to 5 eV, with maxima close to the valence-band maximum and to the conduction-band minimum arising from weakly dispersive bonding and antibonding states in the band structure along Γ−J. The surface states feature also manifest as a shoulder which appears at about 1.5 eV below the VBM, this feature is present up to the S-3 layer and vanished only for the deeper bulk layers. The fact that this feature is related to the surface state due to the π bond can be judged from its disappearance following the termination of the (2×1) with hydrogen. The presence of this feature has also been verified experimentally by photoemission study as a peak at ∼1 eV above the valence band.[34−36]

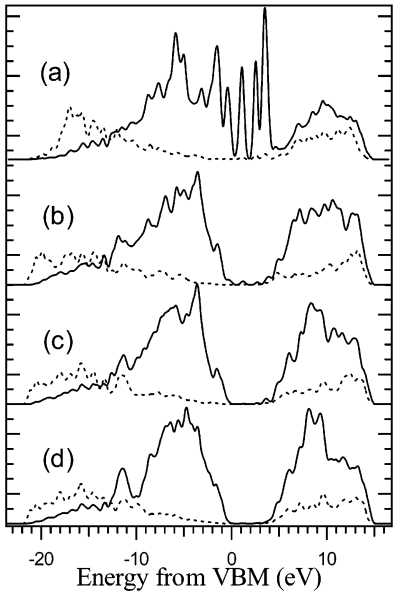

Figure 11. Layered-resolved DOS of clean diamond (2×1) surface showing that the surface states in the gap is concentrated mainly in the (a) top layer, while (b) −1 layer, (c) −2 layers; (d) −3 layers display bulklike DOS states. (—: 2p. - -: 2s.)

The layered-resolved DOS (LDOS) of graphite/diamond in Figure 12 shows that the single layer graphite plane has almost no interaction with the substrate bulk, as can be judged from the similar DOS structure of the first layer substrate carbon (Figure 12b) with that of the clean C(111)-(2×1) surface (Figure 11a). The DOS structure of the single layer graphite in Figure 12a shows the classic 2-D semimetal characteristics. The lower π bonding band is completely filled and the upper π^*-antibonding band is completely empty, with the Fermi level midway between them. In reality, the graphite will not extend indefinitely on the surface but most likely form domains. One possibility is the anchoring of the graphite onto the surface by chemical bonding with adspecies, such as the erect cyclopropylidene structure, which can act as an interfacial structure between the graphite and diamond. The structure of the epitaxial graphite on diamond presents the interesting situation of a semimetal on insulator structure. The erect cyclopropylidene (Figure 4) can act as a bifunctional group to bond between the diamond and graphite and may act as an electron tunnel conduit between the graphite plane and diamond.

For the diamond/quantum chain structure, the LDOS in Figure 13a shows that the first layer carbon exhibits a series of sharp peaks in the valence as well as conduction bands. A gap of 2 eV exists in the valence band between the sp hybrid orbital and the p_y or p_z orbitals. The very sharp peaks are characteristic of the one-dimensional nature of the carbon chain where there

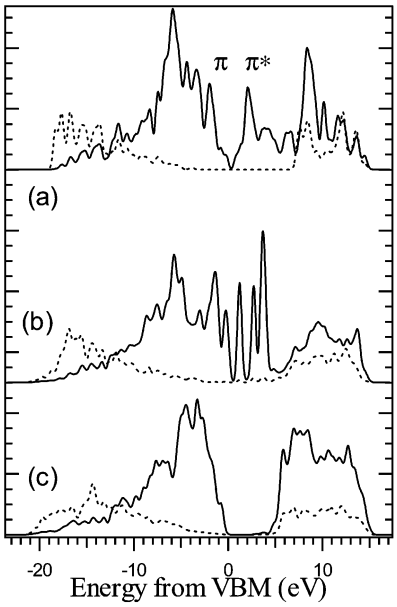

Figure 12. Layered-resolved DOS of C(111) (2 × 1) following the formation of graphite epilayer arising from the assembly of two layers of C_2, showing (a) epilayer graphite on C(111)-(2 × 1) (+ 1 layer); (b) first layer substrate carbon (original surface layer); (c) third layer substrate carbon (−1 layer). (—: 2p. - -: 2s.)

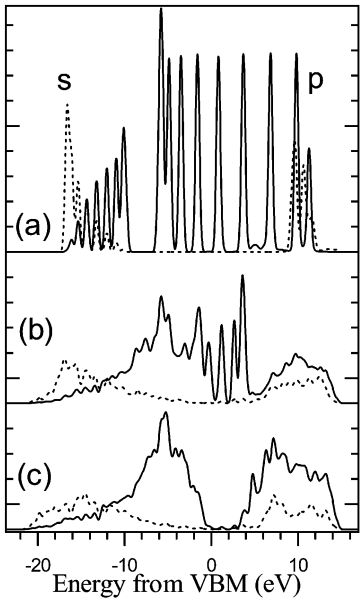

Figure 13. Layered resolved DOS following the assembly of C_2 in an "on-top" fashion on the Pandey chain, giving rise to (a) quantum chain (+1 layer); (b) original substrate layer; (c) −1 layer.

is no interaction with the substrate lattice, and between adjacent chains. Such a situation may arise in reality from the physiosorption of one-dimensional polymeric C_2 chains on the C(111)-(2 × 1) surface where the interaction arises via weak secondary p orbital interactions. The surface layer has no interaction with the substrate, as judged from the similarity between the substrate LDOS in Figure 13b with the clean surface LDOS in Figure 11(a).

On the other hand, strong substrate−adlayer interaction occurs between the first layer chemisorbed C_2 and the Pandey chain, as can be judged from the changes in substrate carbon DOS before and after the chemisorption of C_2 in Figure 14. The LDOS of the chemisorbed C_2 in Figure 14a, when it is adopting the straddled geometry is similar to that of the clean C(111)-(2 × 1), with distinct p−π surface DOS peaks in the gap, indicating

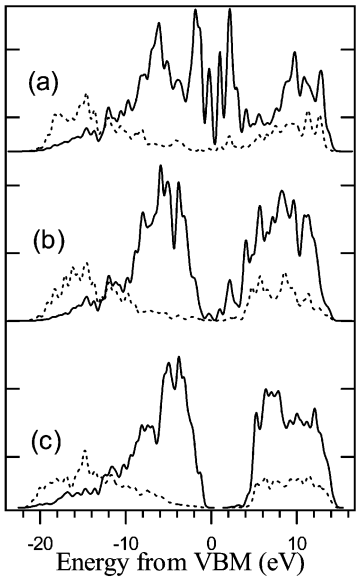

Figure 14. Layered-resolved DOS of (a) chemisorbed C_2 in straddled geometry between Pandey Chain (+1 layer); (b) original substrate carbon (0 layer) and (c) −1 layer. The chemisorbed C_2 in (a) shows π-type surface states in the gap, while the surface states of the substrate carbon in (b) are notably reduced following interaction with the chemisorbed C_2. (—: 2p. - -: 2s.)

that the zigzag chains are electronically equivalent. The interaction of chemisorbed C_2 with the C(111)-(2 × 1) substrate results in the attenuation of the p−π surface DOS peaks *of the substrate carbon* following σ bond formation for surface atoms directly interacting with the C_2, but no complete passivation of the surface states of the substrate carbon occurs as residual intensities can be seen in the gap in Figure 14b. This is due to the charge transfer from the surface chemisorbed C_2 to the first layer substrate.

At the initial stage of acetylene adsorption on the surface, (i.e., when the coverage of C_2H_2 < 50%), two interesting situations exist because we have part of the surface bonded to C_2H_2 directly, while part of it is not bonded (refer Figure 9a.ii). Figure 15a shows that π bonded states can be seen in the LDOS of the chemisorbed acetylene at 50% coverage, this is contrasted with the full sp^3 rehybridization of the acetylene following the conversion into polyethylene. Figure 15b shows that the surface states of the substrate carbon directly interacting with C_2H_2 is attenuated, with a consequent widening of surface gap, indicating that the surface carbon has rehybridized into sp^3-like state. Prominent π and π* peaks are present in the LDOS of the Pandey chain carbon that *has not* reacted with C_2H_2 in Figure 15c. The enhancement of the π and π* peaks, and the shortening of the C−C bonds to 1.375 Å, suggests a stronger π bonding between the Pandey carbon that has not bonded to the C_2H_2. The relaxation of the Pandey carbon atoms that were bonded to the C_2H_2 resulted in a contraction of the bond distances of Pandey carbon atoms not bonded to it. A small gap of ~1 eV has now opened in the LDOS of Pandey carbon atoms that are not bonded to the C_2H_2, where it was absent for the clean C(111)-(2 × 1) surface before. Resonant states in the valence bands of the subsurface layers arising from charge transfer from the surface π states can be seen in Figure 15d,e. For example, the subsurface (−1) layer that is bonded to the Pandey chain not bonded to C_2H_2 shows a resonant state at the valence band maximum, due to charge transfer from the surface π states.

At 100% coverage of the chemisorbed C_2H_2 to form polyethylene, the surface states in the gap of the clean C(111)-(2 × 1) were totally passivated, as shown in Figure 16. Cross-

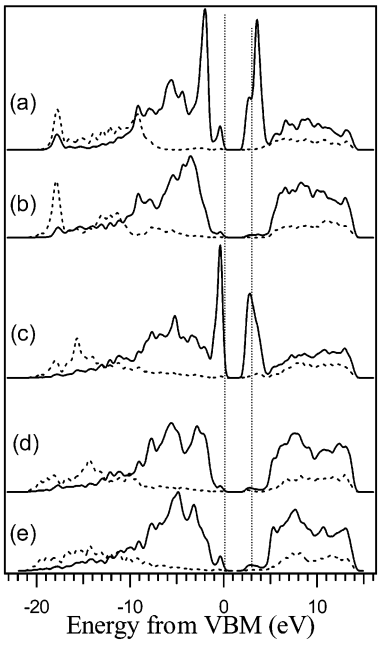

Figure 15. (a) Layered resolved DOS of (a) adsorbed C_2H_2 at 50% coverage; (b) substrate carbon in Pandey chain bonded to C_2H_2 (0 layer); (c) substrate carbon in Pandey chain not bonded to C_2H_2 (0 layer); (d) -1 layer bonded to 0 layer that is bonded to C_2H_2; (e) -1 layer bonded to 0 layer that is not bonded to C_2H_2. (—: 2p. - -: 2s.)

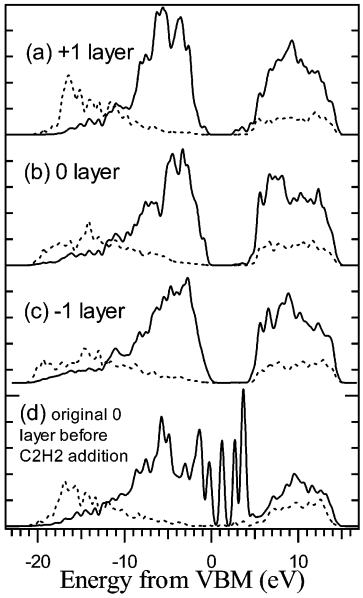

Figure 16. Layered resolved DOS showing the passivation of surface states following the chemisorption of C_2H_2 to form polyetylene. LDOS of (a) C_2H_2 layer (+1 layer); (b) 0 layer; (c) -1 layer. The original surface DOS (0 layer) is shown for reference in (d). (—: 2p. - -: 2s.)

linking via lateral interactions and interaction with the substrate converts the π -bonds in the free acetylene to sp^3 hybridized σ bonds such that no π states remained in the gap region. In other words, the surface becomes almost bulklike with the adsorption of acetylene on the surface. The corresponding surface band structure in Figure 17 shows clearly that the surface band gap region is now devoid of states following passivation by acetylene.

The most stable adsorption configurations for C_2 and C_2H_2 on the reconstructed C(111)-(2 $\times$ 1) face were found to differ in this work. For C_2H_2, a direct on-top insertion into the carbon of the Pandey chain yields a stable cyclobutene structure, and

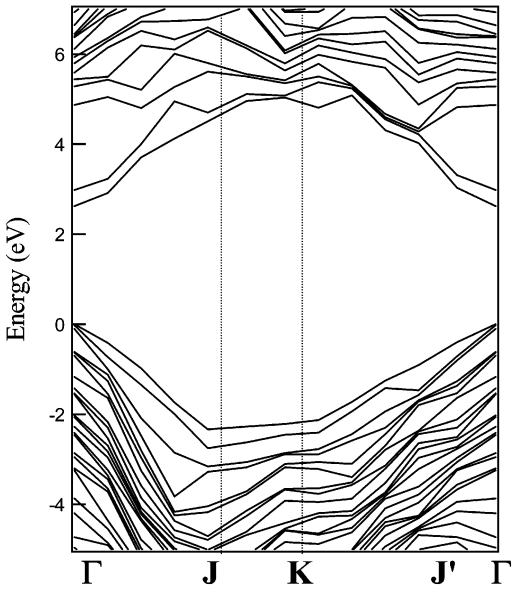

Figure 17. Band structure of the C(111)-(2 $\times$ 1) surface chemisorbed with polyethylene formed by the self-assemby of C_2H_2.

this is the preferred adsorption configuration to the bridging configuration between two Pandey chains. Lateral interaction between the adsorbed C_2H_2 leads to the formation of polyethylene that can run parallel to, and on-top of the Pandey chain. This structure however does not provide a template for the propagation of the C{111} face and inhibits further growth by site-blocking. In the case of C_2, the most stable configuration adopted is the bridging configuration between the two Pandey chains. If a second layer of C_2 adds in a bridging fashion between the two preadsorbed chains on the C(111)-(2 $\times$ 1), self-assembly of the C_2 results in the formation of graphite. This intriguing result is promoted by the structural similarity between the C(111)-(2 $\times$ 1) and graphite. The strong in-plane interaction among C_2 suggests that there is a thermodynamic driving force toward graphitic formation when a hydrogen-poor, C_2-rich gas-feed is utilized for diamond growth on the C(111) substrate.

Conclusion

We performed periodic DFT calculations to derive insights into the degradation mechanism of the slow growing C(111) face under growth conditions employing hydrogen-poor, C_2-rich gas feed. The most stable adsorption site for C_2 is across the Pandey chains of the reconstructed (2 $\times$ 1) surface to generate a [110]-like surface. However the addition of a second layer of C_2 results in the formation of an epitaxial graphite. Therefore addition of C_2 does not provide a facile route for the propagation of the C(111) face due to ready graphitization of the surface. Considerations for C_2H_2 shows that the most stable configuration is the "on-top" site of the Pandey chain. The unique symmetry of the zigzag chain on the C(111)-(2 $\times$ 1) provides a molecular template that favors the lateral interaction between the chemisorbed C_2H_2, leading to self-assembly of polyethylene that runs parallel to the chain. Our results suggest that it is possible to form ordered organic monolayer by the highly specific interaction between the π bonds of unsaturated organic species and the π bonds on the diamond Pandey chains.

Acknowledgment. The author K. P. Loh acknowledges the support of NUS academic research fund R-143-000-162-112 for this project.

References and Notes

(1) Gruner, G. *Density Waves in Solids*; Addison-Wesley: Reading, 1994.
(2) Tanaka, K. *Jpn. J. Appl. Phys*. **1993**, *32*, 1389.
(3) Bertel, E.; Lehman, J. *Phys. Rev. Lett*. **1998**, *80*, 1497.
(4) Chen, X.; Wu, F.; Zhang, Z.; Lagally, M. G. *Phys. Rev. Lett*. **1994**, *93*, 850.
(5) Miki, K. et. al. *Surf. Sci*. **1999**, *421*, 397.
(6) Hara, S.; Misawa, S.; Yoshida, S.; Aoyagi, Y. *Phys. Rev. B* **1994**, *50*, 4548.
(7) Yeom, H. W. et al. *Phys. Rev. B* **1997**, *56*, R15525.
(8) Widdra, W. et al. *Phys. Rev. Lett*. **1998**, *80*, 4269.
(9) Zhou, D.; McCauley, T. G.; Qin, L. C.; Krauss, A. R.; Gruen, D. M. *J. Appl. Phys*. **1998**, *83*, 540.
(10) Zhou D.; Gruen, D. M.; Qin, L. C.; McCauley, T. G.; Krauss, A. R. *J. Appl. Phys*. **1998**, *84*, 1981.
(11) Gruen, D. M.; Liu, S. Z.; Krauss, A. R.; Luo, J. S.; Pan, X. Z. *Appl. Phys. Lett*. **1994**, *64*, 1502.
(12) Horner, D. A.; Curtis, L. A.; Gruen, D. M. *Chem. Phys. Lett*. **1995**, *233*, 245.
(13) Horner, D. A.; Curtis, L. A.; Gruen, D. M. *J. Phys. Chem*. **1996**, *100*, 11654.
(14) Goyette, A. N.; Lawler, J. E.; Anderson, L. W.; Gruen, D. M.; MaCauley, T. G.; Zhou, D.; Krauss, A. R. *Plasma Sources Sci. Technol*. **1998**, *7*, 149.
(15) Lin, Q.; Hamers, R. *J. Am. Chem. Soc*. **1997**, *119*, 7593.
(16) Lin, Q.; Hoffman, R. *J. Am. Chem. Soc*. **1995**, *117*, 4082.
(17) Lin, T.; Yu, G. Y.; Wee, A. T. S.; Shen, Z. X.; Loh, K. P. *Appl. Phys. Lett*. **2000**, *77*, 2692.
(18) Rego, C. A.; May, P. W.; Henderson, C. R.; Ashfold, M. N. R.; Rosser, K. N.; Everitt, N. M. *Diamond Related Mater*. **1995**, *4*, 770.
(19) Ricacardi, C.; Barni, R.; Fontanesi, M.; Tosi, P. *Chem. Phys. Lett*. **2000**, *66*, 329.
(20) Horner, D. A.; Curtiss, L. A.; Gruen, D. M. *Chem. Phys. Lett*. **1996**, *223*, 243.
(21) Redfern, P. C.; Horner, D. A.; Curtis, L. A.; Gruen, D. M. *J. Phys. Chem*. **1996**, *100*, 11654.
(22) Gruen, D. M.; Redfern, P. C.; Horner, D. A.; Zapol, P.; Curtiss, L. A. *J. Phys. Chem. B*. **1999**, *103*, 5459.
(23) Pandey, K. C. *Phys. Rev. Lett*. **1981**, *47*, 1913.
(24) Kern, G.; Hafner, J.; Kresse, G. *Surf. Sci*. **1996**, *366*, 464.
(25) Kress, C.; Fiedler, M.; Schmidt, W. G.; Beehstedt, F. *Surf. Sci*. **1995**, *331*, 1152.
(26) Payne, M. C.; Teter, M. P.; Allan, D. C.; Arias, T. A.; Joannopoulos, J. D. *Rev. Mod. Phys*. **1992**, *64*, 1045.
(27) Milman, V.; Winker, B.; White, J. A.; Pickard, C. J.; Payne, M. C.; Akhmatskaya, E. V.; Nobes, R. H. *Int. J. Quantum Chem*. **2000**, *77*, 895.
(28) Vanderbilt, D. *Phys. Rev. B* **1990**, *41*, 7892.
(29) Monkhorst, H. J.; Pack, J. D. *Phys. Rev. B* **1976**, *13*, 5188.
(30) Polak, E. *Computational Methods in Optimization*; Academic: New York, 1971; p 56ff.
(31) Perdew J. P.; Wang Y. *Phys. Rev. B*, **1992**, *45*, 13244.
(32) Ueno, K.; Sakurai, M.; Koma, A. *J. Cryst. Growth* **1995**, *150*, 1180.
(33) Forbeau, I.; Themlin, J. M.; Debever, J. M. *Phys. Rev. B* **1998**, *58*, 16396.
(34) Himpsel, F. J.; van der Veen, J. F.; Eastman, D. E. *Phys. Rev. B* **1980**, *22*, 1967.
(35) Himpsel, F. J.; Eastman, D. E.; Heimann, P.; van der Veen, J. F. *Phys. Rev. B* **1981**, *24*, 7270.
(36) Pate, B. B.; Hecht, M. H.; Binns, C.; Lindau, I.; Spicer, W. E. *J. Vac. Sci. Technol*. **1982**, *21*, 364.